

# Spectroscopic ellipsometry studies of amorphous PZT thin films with various Zr/Ti stoichiometries

SHENGHONG YANG\*

Department of Physics, Fudan University, Shanghai, 200433, People's Republic of China  
E-mail: shenghongyang@163.com

DANG MO

State Key Laboratory of Ultrafast Laser Spectroscopy and Department of Physics, Zhongshan University, Guangzhou 510275, People's Republic of China

XINGGUI TANG

Laboratory of Functional Inorganic Materials, Chinese Academy of Science, 1295, Ding Xi RD., Shanghai, 200050, People's Republic of China

Amorphous stoichiometric  $\text{Pb}(\text{Zr}_x\text{Ti}_{1-x})\text{O}_3$  (PZT) thin films with various values of  $x$  were deposited on Si(100) substrates by the sol-gel technique. The influence of Ti content on the optical properties was studied by spectroscopic ellipsometry (SE) in the UV-visible region. Using a four-phase fitting model, the refractive index  $n$  and extinction coefficient  $k$  was obtained by analyzing the SE spectra. The optical band gap energies  $E_g$  for these films were reported under the assumption of a direct band-to-band transition. It has been found that the refractive index, extinction coefficient and band gap energy of the films were functions of the film compositions. The refractive index of the PZT films increases linearly with increasing Ti content. On the other hand, the optical band gap energy of the PZT films decreases with increasing Ti content. © 2002 Kluwer Academic Publishers

## 1. Introduction

Lead zirconate titanate  $\text{Pb}(\text{Zr}_x\text{Ti}_{1-x})\text{O}_3$  (PZT) is a very interesting ferroelectric material because of its pronounced pyroelectric, ferroelectric and electro-optic properties [1, 2]. Thin PZT films have been successfully employed in the fabrication of non-volatile memory [2], infrared (IR) optical field effect transistor [3] and electro-optic switches and modulators [4]. The stoichiometry of PZT thin films can be varied to produce different properties. Although many studies on the structural and electrical properties of these films have been reported [1, 2, 5], very limited reports exist on their optical properties. Xu *et al.* [6] found that some amorphous PZT thin films exhibit excellent ferroelectric-like properties, such as hysteresis loops, stable pyroelectric currents, and piezoelectric resonance peaks in the dielectric spectrum. Recently, a theoretical explanation for the ferroelectric-like properties of amorphous PZT thin films was reported [7]. These excellent properties show that further studies, including optical measurements, need to be performed for the amorphous PZT films. However, there is little data on the optical constant spectra of amorphous PZT films in a wide wavelength range.

As for the optical research on PZT films, it has been studied by ellipsometric technique by Trolier-McKinstry *et al.* [8, 9]. In their work, however, most

samples used are crystalline, and the measured wavelength range is rather narrow: 400–650 nm or 300–700 nm. So the spectra of refractive index  $n$  show monotonic behavior and the spectra of extinction coefficient  $k$  has not been given. The optical properties of amorphous PZT thin films are of particular importance for e.g., optical modulator and optical display device. The optical characterization also gives valuable insight into the structural parameters of the film such as packing density, thickness, and surface roughness.

In this paper, we report on SE measurements of the key optical constants (refractive index, extinction coefficient) for the amorphous PZT thin films. SE is a non-destructive and sensitive optical technique that has been widely recognized as a reliable tool for characterizing optical properties of thin films [10]. In the analysis of the SE spectra, a four-phase model was employed, in which the optical properties of amorphous PZT films were represented by the Forouhi-Bloomer model [11]. Our main objective was to determine the optical properties of amorphous PZT thin films as a function of compositions.

## 2. Experimental details

### 2.1. Sample preparation

In this work, amorphous  $\text{Pb}(\text{Zr}_x\text{Ti}_{1-x})\text{O}_3$  thin films with various values of  $x$  ( $x = 0.9, 0.8, 0.7, 0.5, 0.4$ )

\*Author to whom all correspondence should be addressed.

were prepared on Si(100) substrates by the sol-gel method.

High-purity lead acetate trihydrate  $\text{Pb}(\text{CH}_3\text{COO})_2 \cdot 3\text{H}_2\text{O}$ , titanium alkoxide ( $\text{Ti}(\text{OC}_3\text{H}_7)_4$ ), and zirconium-*n*-propoxide  $\text{Zr}(\text{O}(\text{CH}_2)_2\text{CH}_3)_4$  were used as starting materials; methanol  $\text{CH}_3\text{OH}$  and 2-methoxyethanol  $\text{C}_3\text{H}_8\text{O}_2$  were selected as solvents, and acetic acid  $\text{CH}_3\text{COOH}$  was used as stabilizing agent. Lead acetate trihydrate was dissolved in methanol at  $70^\circ\text{C}$  under stirring, 10 mol% extra lead acetate trihydrate was added, then cooled to room temperature. Zirconium-*n*-propoxide and titanium alkoxide were mixed in a de-

sired ratio of Zr/Ti, e.g.,  $\text{PbZr}_{0.9}\text{Ti}_{0.1}\text{O}_3$  (90/10), then dissolved in 2-methoxyethanol at room temperature under stirring. These two solutions were mixed in a reaction flask under stirring at  $70^\circ\text{C}$  for 2 h. Using acetic acid to prevent partial hydrolysis, the concentration of the final solution was adjusted to 0.3 M, and pH value was 3–4. The solution that is usually called the precursor solution was colorless transparent. Before the spin-coated, the silicon substrates were ultrasonically cleaned with acetone and ethanol, then etched for 1 min in 2% HF water solution in order to remove the surface oxide. The precursor solution was spin-coated directly on an Si(100) substrate to form a uniform wet film at room temperature. The rotation speed and the spin time were fixed at 400 rpm and 30 s, respectively. Wet films were pre-annealed at  $350^\circ\text{C}$  in air for 10 min. Then the films were annealed in an oxygen atmosphere at  $450^\circ\text{C}$  for 10 min by rapid thermal annealing (RTA).

The microstructures of the PZT thin films were examined by a D/Max-RC x-ray diffractometer with  $\text{Cu-K}\alpha$  radiation. Fig. 1 shows the typical x-ray diffraction (XRD) pattern of these PZT thin films. The film annealed at  $450^\circ\text{C}$  for 10 min with RTA is amorphous according to the XRD pattern shown in Fig. 1.

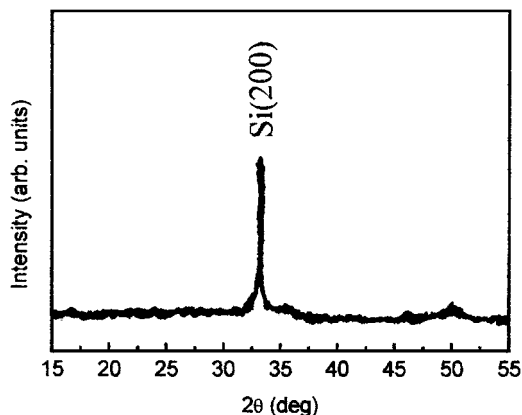


Figure 1 Typical XRD pattern of PZT thin films deposited on Si(100) substrate annealed at  $450^\circ\text{C}$  for 10 min with RTA.

## 2.2. Ellipsometric experiment

A high precision photometric ellipsometer was used in the characterization of the PZT thin films. Because the details on SE can be found in the literature [10], only

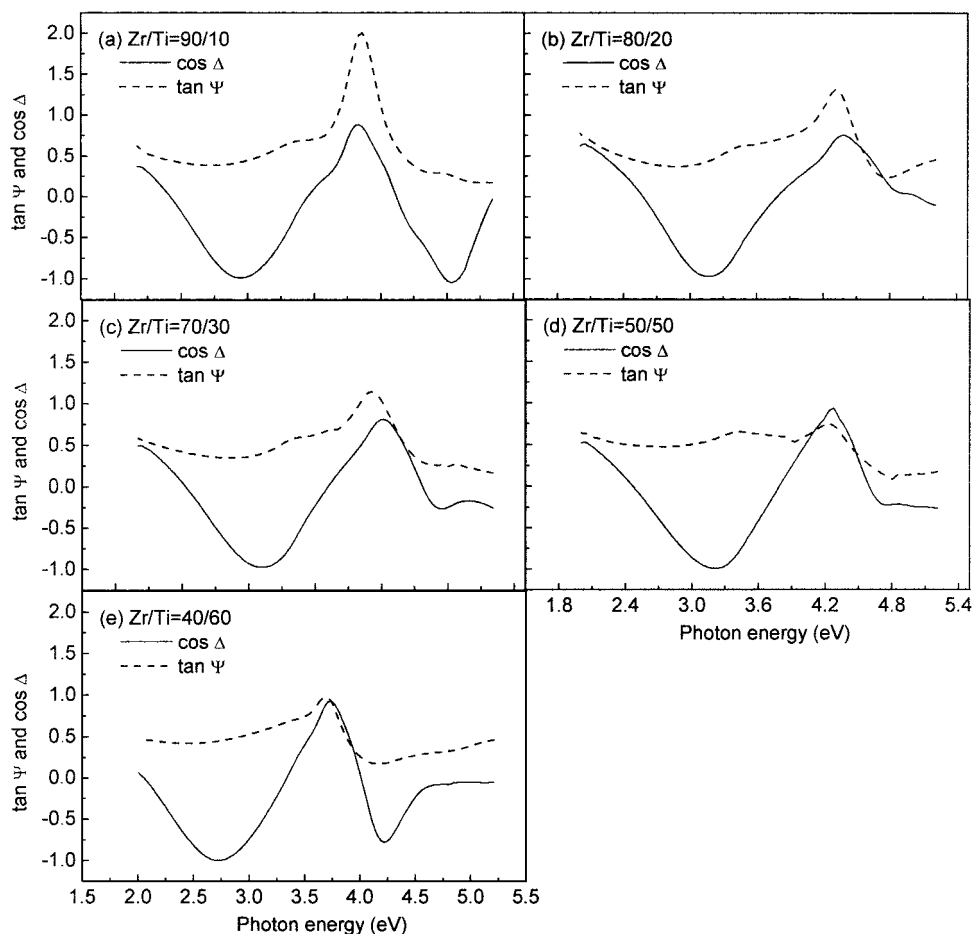


Figure 2 Ellipsometric spectra of amorphous PZT thin films with different Zr/Ti ratios. (a) Zr/Ti = 90/10, (b) Zr/Ti = 80/20, (c) Zr/Ti = 70/30, (d) Zr/Ti = 50/50, (e) Zr/Ti = 40/60.

TABLE I Summary of fitting parameters for a series of amorphous PZT films examined in this study

Zr/Ti ratio	Thickness (nm)		Fitting parameters				
	Determined by SE	Determined by profilometer	A	B	C	D	$n_\infty$
90/10	115.7	120	0.078	10.82	30.87	2.99	1.90
80/20	103.8	109	0.12	8.93	21.99	3.17	1.97
70/30	103.8	110	0.096	9.33	22.99	3.12	2.02
50/50	86.2	89	0.90	9.73	24.75	2.95	2.23
40/60	99.7	102	0.049	10.11	25.77	2.87	2.26

a brief description is given here. In ellipsometry, the object is to measure the ratio of the complex Fresnel reflection coefficients,  $\rho$ , where

$$\rho = r_p/r_s = \tan \Psi \exp(i\Delta). \quad (1)$$

The quantity  $r_p(r_s)$  is the Fresnel reflection coefficients for light polarized parallel (perpendicular) to the plane of incidence, and  $\Psi$  and  $\Delta$  are the traditional ellipsometric angles. Note that both  $r_p$  and  $r_s$  contain information on the optical and structural properties of the sample. The  $\tan \Psi$  and  $\cos \Delta$  are measured in a photometric rotating-analyser ellipsometer, by Fourier analysis of curves of the light intensity vs. the azimuthal angle of the rotating analyzer.

All the SE measurements were carried out at room temperature in the 238–618 nm (corresponding to 5.2–2.0 eV) wavelength range at 2-nm intervals, with operated at an angle of incidence of  $70^\circ$  and an azimuthal angle of the polarizer of  $45^\circ$ . The thicknesses of the films were measured by profilometer. The results were shown in Table I. The thicknesses derived from profilometer were about in the range of 90–110 nm.

### 3. Results and discussion

The SE spectra for amorphous  $\text{Pb}(\text{Zr}_x\text{Ti}_{1-x})\text{O}_3$  thin films with  $x$  from 0.9 to 0.4 are shown in Fig. 2a–e. In the lower energy range, the spectra exhibit oscillations. This is only due to the interference effect of light, and this indicates that the films are transparent. The oscillating frequency depends on the thickness of the film. Generally, the thicker is the film, the higher is the frequency.

The optical constants derived from the ellipsometric parameters of  $\tan \Psi$  and  $\cos \Delta$  are analysed by a four-phase model (air/PZT + voids/PZT/substrate), as shown in Fig. 3. The presence of a rough surface layer is a common feature for sol-gel-derived oxide thin films [12]. The rough surface layer was modeled using a Bruggeman effective medium approximation [13] consisting of voids and PZT. There are a large number of voids with almost 40% of air volume in the rough surface layer (layer of PZT + voids). The optical constants of PZT were parameterized using the Forouhi-bloomer models, given by [11]

$$n(E) = n_\infty + \frac{A(-B^2E + 2DBE - 2D^2E + 2CE + D^2B + BC - 4DC)}{\sqrt{4C - B^2 \cdot (E^2 - BE + C)}} \quad (2)$$

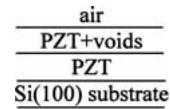


Figure 3 Schematic diagram of the film structure used in SE fitting.

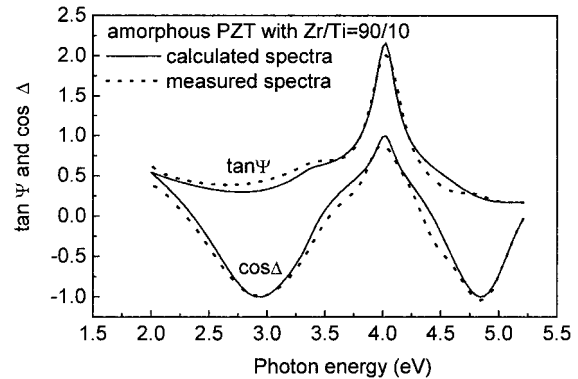


Figure 4 Experimental spectra (dotted line) and calculated spectra (solid line) of  $\text{PbZr}_{0.9}\text{Ti}_{0.1}\text{O}_3$  films with Zr/Ti = 90/10.

$$K(E) = \frac{A(D - E)^2}{E^2 - BE + C} \quad (3)$$

where  $E$  is the photon energy and the fitting parameters are  $A$ ,  $B$ ,  $C$ ,  $D$  and  $n_\infty$ . The optical constants of Si(100) were taken from Ref. [14]. With the help of simulated annealing optimization [15], the fitting parameters as well as the film thicknesses were determined by fitting the ellipsometric spectra. Fig. 4 shows a fit for amorphous  $\text{PbZr}_{0.9}\text{Ti}_{0.1}\text{O}_3$  thin film, and clearly, the fit shown in Fig. 4 is a good fit. Table I shows the details of the fitting parameters obtained from the fit for five amorphous PZT films.

As shown in Table I, the thicknesses of PZT films obtained by SE closely matches those obtained by profilometer. Therefore, it is verified that our model adequately describes the measured data. Fig. 5 shows the refractive index ( $n$ ) and extinction coefficient ( $k$ ) obtained from the fitted parameters for five amorphous PZT films. From Fig. 5, we find that the optical constants spectra of all PZT films show a high refractive index ( $n = 1.7$ – $2.9$ ) in the UV-visible region as well as the fundamental absorption edge in the near ultraviolet region. The refractive index first increased and then decreased as the photon energy increased from 2.0 to 5.2 eV. The extinction coefficient of the films increases as photon energy increases, consistent with Kramers-Kronig relations. The extinction coefficients are very small at lower photon energy, where the films are nearly transparent. On the other hand, we also find different values of the refractive index and extinction coefficient due to the different compositions. The refractive index of the amorphous PZT films increases linearly with increasing Ti content. This is the same as PLZT ceramics, whose refractive index is largely controlled by the Zr/Ti ratio [16]. A higher Ti content in

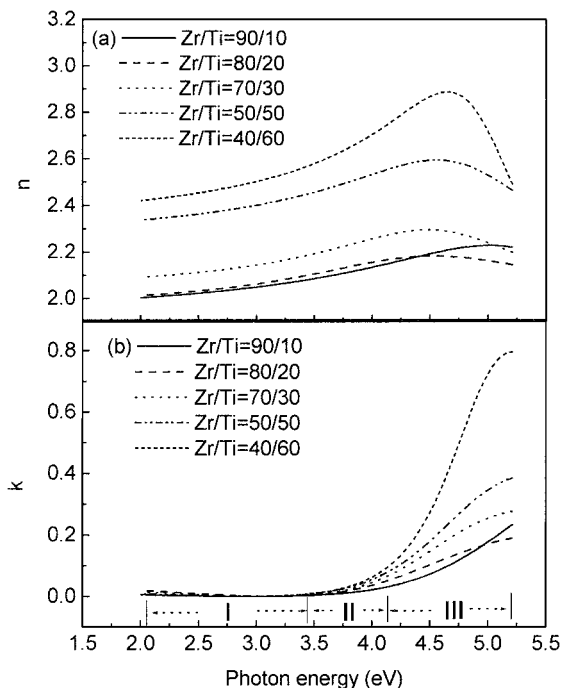


Figure 5 Optical constants ( $n$  and  $k$ ) of amorphous PZT films with different Zr/Ti ratios.

PZT films enhances the formation of larger and more closely packed crystals. The increase of the refractive index with increasing Ti content can be partly attributed to the increase of the packing density. This change of refractive index was also observed by Trolier-McKinstry *et al.* [8] for polycrystalline PZT films.

The extinction coefficient ( $k$ ) spectra for the PZT thin films with different Ti content are also shown in Fig. 5. From the spectral relationship between extinction coefficient and photon energy, the extinction coefficient of PZT thin films can be divided into three regions. Region I: the low-energy of the spectra ( $E = 2.0\text{--}3.5$  eV, below the fundamental band gap energy  $E_g$ ); region II and III: the high-energy regions ( $E = 3.5\text{--}4.2$  and  $4.2\text{--}5.2$  eV, above  $E_g$ ). No obvious absorption is found below the fundamental band gap energy  $E_g$ . The extinction coefficient is near to zero except when the photon energy increased close to the band gap energy. The dispersion in region II and III are due to the transition from the valance band to the conduction band, or a transition from a band to an impurity level. It is interesting that the extinction coefficient increases as the Ti content of amorphous PZT thin films increasing in the region II and III. The values of the extinction coefficient, as we know, result from the absorption and grain scattering when the photon wavelength is equivalent to the grain size in the high-energy region. The possibility of scattering of the grains increases as the Ti content increases, which can also be attributed to the increase of grain size and surface density of the films. The extinction coefficient near the fundamental band gap energy is not zero because of the noise, and the results demonstrated that some other absorption is present in addition to the fundamental transition.

The optical band gap energy  $E_g$  of amorphous PZT films were calculated by considering a direct allowed electronic transition between the highest occupied state

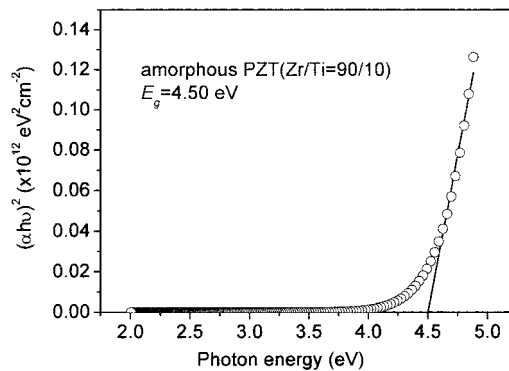


Figure 6 Plot of  $(\alpha h\nu)^2$  versus  $h\nu$  for  $\text{PbZr}_{0.9}\text{Ti}_{0.1}\text{O}_3$  films, the optical band gap energy  $E_g$  is deduced from extrapolation of the straight line to  $(\alpha h\nu)^2 = 0$ .

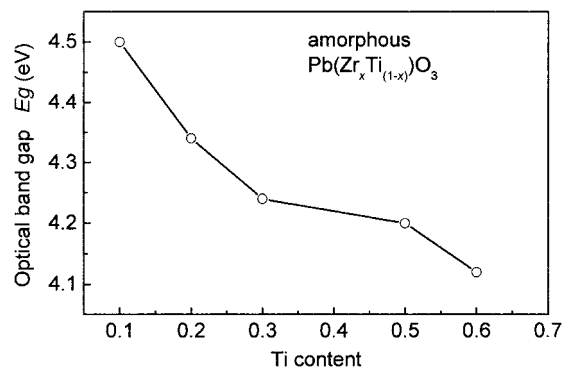


Figure 7 Optical band gap energies of amorphous PZT films as a function of Ti contents ( $x$  denotes the content of Zr).

of the valance band and the lowest unoccupied state of the conduction band when a photon of energy,  $h\nu$ , falls on the material. In this case, the absorption coefficient  $\alpha$  is related to the optical band gap energy  $E_g$  as [17]

$$(\alpha h\nu)^2 = \text{Constant} \cdot (h\nu - E_g), \quad (4)$$

where

$$\alpha = 4\pi k/\lambda, \quad (5)$$

the  $E_g$  values are therefore determined by extrapolating the linear portion of the plot relating  $(\alpha h\nu)^2$  versus  $h\nu$  to  $(\alpha h\nu)^2 = 0$ . As an example, Fig. 6 shows the optical band gap energy for amorphous  $\text{PbZr}_{0.9}\text{Ti}_{0.1}\text{O}_3$  films,  $E_g = 4.50$  eV.

The  $E_g$  value of amorphous PZT films is a composition-dependent parameter. Fig. 7 shows the variation of  $E_g$  with Ti content in PZT films. The  $E_g$  value is found to decrease from 4.50 to 4.12 eV with increasing Ti content from 0.1 to 0.6. The decrease in  $E_g$  denotes the change in the structure. This is in agreement with the structural experimental results of PZT films reported in the literature [18]. Sreeivas *et al.* [19] also have reported that the optical absorption edge is a very strong function of film compositions. These results are in agreement with our results. When Zr is a substitute for Ti in the PZT films,  $\text{Zr}^{2+}$  ions will occupy the lattice site of the  $\text{Ti}^{2+}$  ions, which will enhance the coupling effect between the  $\text{Pb}^{2+}$  and  $\text{O}^{2-}$  ions because the effect of the Zr-O bond is stronger than that of the Ti-O

bond. Furthermore, the lattice parameters will decrease with increasing Zr content in the PZT thin films, due to the difference in radii of the  $\text{Ti}^{2+}$  ions ( $r = 0.09$  nm) and  $\text{Zr}^{2+}$  ions ( $r = 0.086$  nm). It is therefore more favorable to fabricate films with a higher packed density and less voids. These facts may induce the shift of  $E_g$  values.

#### 4. Conclusions

In conclusion, the optical properties of amorphous  $\text{Pb}(\text{Zr}_x\text{Ti}_{1-x})\text{O}_3$  thin films with various values of  $x$  coated on Si(100) substrates by the sol-gel method have been investigated by the spectroscopic ellipsometry in the UV-visible region. Using a four-phase fitting model, the spectra of the optical constants and the band gap energy  $E_g$  have been determined by means of optimization. Our studies show a strong dependence of the optical constants and optical band gap energy on Zr/Ti ratios in the deposited films. The thickness values obtained from SE measurement compare well with the surface profilometer data. The refractive index for PZT films increases as the Ti content in PZT films is increased. The optical band gap energies have been found to decrease from 4.50 to 4.12 eV as the Ti content in the films is increased from 0.1 to 0.6.

#### Acknowledgment

This work was supported by the National Natural Science Foundation of China under Grant No. 19874081.

#### References

1. J. F. SCOTT and C. A. PAZ DE ARAJUO, *Science* **246** (1993) 1400.

2. Y. XU, in "Ferroelectric Materials and Their Applications" (North-Holland, Amsterdam, 1991) p. 206.
3. K. IJIMA, Y. TOMITA, R. TAKAYAMA and I. UEDA, *J. Appl. Phys.* **60** (1986) 361.
4. H. ADACHI, T. MITSUYU, O. YAMAZAKI and K. WASA, *ibid.* **60** (1986) 736.
5. D. L. POLLA and L. F. FRANCIS, *Annu. Rev. Mater. Sci.* **28** (1998) 263.
6. Y. XU, C. H. CHENG and J. D. MACKENZIE, *J. Non-Cryst. Solids* **176** (1994) 1.
7. Y. XU and J. D. MACKENZIE, *ibid.* **246** (1999) 136.
8. S. TROLIER-MCKINSTRY, H. HU, S. B. KRUPANIDHI, P. CHINDAUDOM, K. VEDAM and R. E. NEWNHAM, *Thin Solid Films* **230** (1993) 15.
9. S. TROLIER-MCKINSTRY, J. CHEN, K. VEDAM and R. E. NEWNHAM, *J. Amer. Ceram. Soc.* **78** (1995) 1907.
10. R. M. A. AZZAM and N. M. BASHARA, in "Ellipsometry and Polarized Light" (North-Holland, Amsterdam, 1977) p. 89.
11. A. R. FOROUHI and I. BLOOMER, *Phys. Rev. B* **34** (1986) 7018.
12. M. M. RAHAM, G. L. YU, K. M. KRISHNA, T. SOGA, J. J. WANTANABLE, T. JIMBO and M. UMENO, *Appl. Opt.* **37** (1998) 691.
13. D. A. G. BRUGGEMAN, *Ann. Phys. Leipzig* **24** (1933) 636.
14. G. E. JELLISON, JR., *Opt. Mater.* **1** (1992) 41.
15. S. KIRKPATRICK, C. D. GELATT and M. P. VECCHI, *Science* **220** (1983) 671.
16. P. D. THAACHER, *Appl. Opt.* **16** (1977) 3210.
17. J. C. TAUC, in "Amorphous and Liquid Semiconductor" (Plenum Press, New York, 1974) p. 159.
18. G. H. YI, Z. WU and M. SAYER, *J. Appl. Phys.* **64** (1988) 2717.
19. K. SREENIVAS, M. SAYER and P. GARRETT, *Thin Solid Films* **172** (1989) 251.

Received 20 November 2001

and accepted 3 June 2002